AMERICAN JOURNAL of PHYSICS

Volume 80, No. 1, January 2012

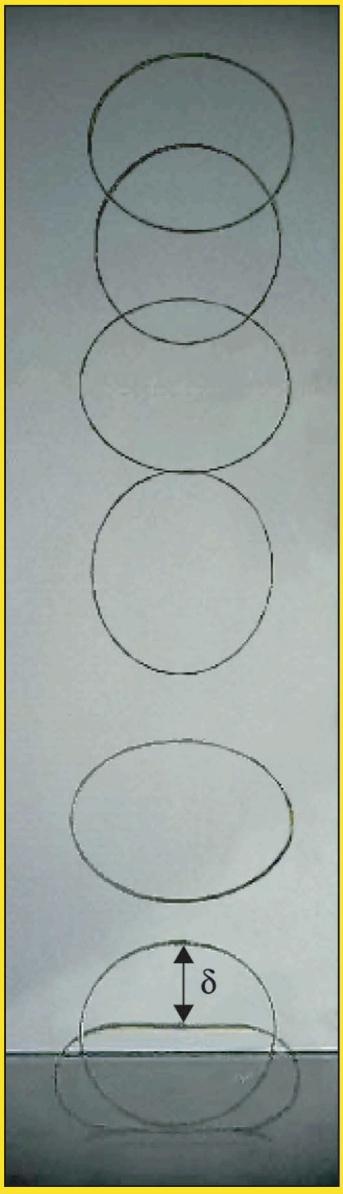

A PUBLICATION OF THE AMERICAN ASSOCIATION OF PHYSICS TEACHERS

Available online—visit http://aapt.org/ajp

Jumping hoops

Eunjin Yang and Ho-Young Kim[a)]
School of Mechanical and Aerospace Engineering, Seoul National University, Seoul 151-744, Korea

(Received 24 April 2011; accepted 17 August 2011)

We investigate the dynamics of an elastic hoop as a model of the jumps of small insects. During a jump the initial elastic strain energy is converted to translational, gravitational, and vibrational energy, and is dissipated by interaction with the floor and the ambient air. We show that the strain energy is initially divided into translational, vibrational, and dissipation energies with a ratio that is constant regardless of the dimension, initial deflection, and the properties of a hoop. This novel result enables us to accurately predict the maximum jump height of a hoop with known initial conditions and drag coefficient without resorting to a numerical computation. Our model reduces the optimization of the hoop geometry for maximizing the jump height to a simple algebraic problem.
[DOI: 10.1119/1.3633700]

I. INTRODUCTION

Jumping is used by animals as an efficient means of locomotion to escape predators, to catch prey, to increase their speed, or to launch into flight.[1] Small insects such as froghoppers,[1] crickets,[2] fleas,[3] grasshoppers,[4] and water striders[5,6] are able to jump many times their body lengths. Their jumps are powered by muscles that rapidly release stored elastic energy through a latch mechanism.[4] The major research foci of the field have been on the anatomical structure of organs associated with jumping,[9–11] the jump kinematics,[2,12,13] and the power exerted by the muscle that drives the jumps.[4,14]

Interest in the jumping of small objects is increasing outside biology. Inspired by the superior maneuverability of those insects, biomimetic robots, which mimic the structures, functions and designs of living creatures, are being developed with the goal to jump on land[7] and water.[8] Optimizing the robot design to maximize the jump height is essential, given the constraints on material properties, size, and weight.

In contrast, the jump dynamics of small elastic objects have drawn little interest so far.[12] In this paper, we analyze the dynamics of a model jumper, an elastic hoop, because of its simple geometry, ease of fabrication, and immediate implications for biomimetic robots.[7] Circular-shaped robots have many advantages such as their structural stability and superior terrestrial mobility.[7] Despite the long history of studying the dynamics of thin and thick hoops,[15–20] the jumps of the hoop have been seldom treated from a strictly mechanical point of view. As a consequence, questions regarding the energy efficiency of the jumps of the hoop (the ratio of the translational kinetic energy to the initially stored strain energy) and the amount of energy wasted due to the interaction with the substrate, the hoop vibration, and the effects of air drag are still unanswered. We address these questions and obtain the maximum jump height and the optimum design by a combination of experiments and the theory of elasticity.

II. EXPERIMENTS

To measure the jump height of an elastic hoop off a rigid substrate, we made hoops of steel (SK5 carbon steel) with Young's modulus $Y = 196$ GPa, density $\rho = 8.00 \times 10^3$ kg/m^3, and yield stress[15] $\sigma_y = 612$ MPa. We also used polyimide films (Dupont Kapton) with $Y = 3.55$ GPa, $\rho = 1420$ kg/m^3, and $\sigma_y = 69.0$ MPa. The thickness τ of the hoop ranges between 75 and 125 μm, and the radius (the average of the inner and outer radius in the undeformed state) R is between 10 and 30 mm; the width is fixed to $w = 3$ mm [see Fig. 1(a)]. We tested glass, acrylic, and aluminum and found that the jumps of the hoops are insensitive to the rigid substrate material (the maximum jump height differed by at most $\pm 1\%$ depending on the material). In contrast, when the substrates are very soft such as a flexible polymer membrane, the deformation of the substrate has a great influence on the dynamics of the hoop. All the data in this paper are for a glass substrate.

A circular hoop resting on the substrate is bent by a sharp tip which is rapidly pulled back horizontally by a spring to let go of the hoop without interfering with its motion. We visualized the resulting motion of the hoop using a high-speed camera (Photron FASTCAM APX-RS) at the frame rate 3000 s^{-1} as shown in Fig. 1(b). The location and shape of the hoop were obtained by digitizing the image, which consists of 512×720 pixels. The object size is calibrated by imaging a ruler with the identical imaging setup. After release, the hoop starts to recover its circular shape while maintaining contact with the substrate ($t = 0$–5 ms) (see Fig. 2). It disengages from the substrate after reaching a perfect circle ($t = 5$ ms). While in the air, the hoop vibrates between oblate and prolate shapes. By measuring the maximum height H reached by the hoops for various values of R, τ, and initial deflection δ, we found that the hoop jumps higher as the radius is decreased and as the thickness and the initial deflection are increased. The results are explained in the following.

III. JUMPING WITHOUT DRAG

We first consider what happens to the initial elastic strain energy E_b due to bending when the hoop jumps. After release, the hoop's elastic energy is partially imparted to the substrate, the amount of which is denoted by E_s. The rest is used to set the hoop in motion. Two different modes of the hoop motion occur: translation and vibration. Conservation of energy implies that $E_b = E_s + E_{t,0} + E_{v,0}$, where $E_{t,0}$ and $E_{v,0}$ refers to the initial translational and initial vibrational kinetic energy, respectively. $E_{t,0}$ is converted to three forms of

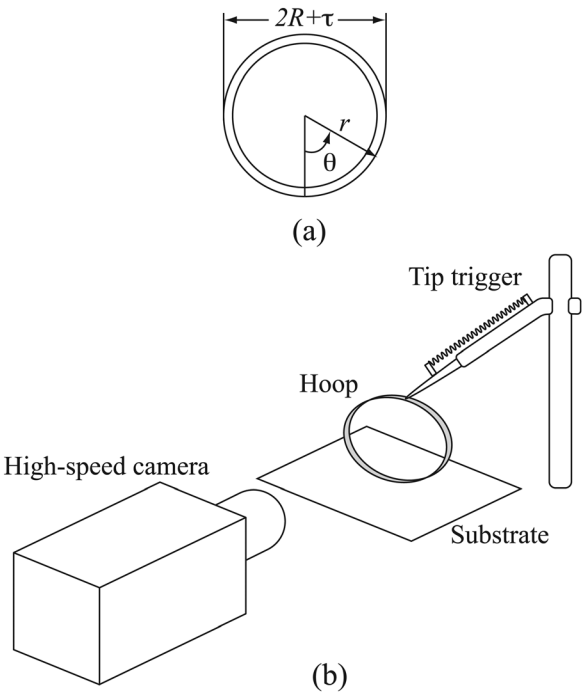

Fig. 1. (a) The geometry of an elastic hoop. (b) The experimental apparatus.

energy during ascent, the translational energy E_t, the gravitational potential energy $E_g = mgh$, and the energy loss due to air drag E_d, where m and h are the mass and the instantaneous height of the hoop, respectively, and g is the gravitational acceleration. At the highest point, where $E_t = 0$ and $h = H$, energy conservation can be written as $E_b = E_s + E_g + E_d + E_{v,0}$.

The elastic strain energy of a hoop can be found from the linear relation between the compressive force F and the resulting deformation δ: $F = k\delta$, where $k = \eta Y w \tau^3/R^3$ with $\eta = \pi/[3(\pi^2-8)] = 0.56$.[15] We obtain $E_b = k\delta^2/2 = 0.28 Y w \tau^3 \delta^2/R^3$. By measuring F and δ, we find the linear relation to hold well beyond the geometrically linear regime (that is, small deformations compared with the hoop length) until the upper and lower segments of the hoop touch each other, that is, $\delta = 2R - \tau$.

To find the energy associated with the motion of the hoop, we write the velocity of the thin hoop as $\mathbf{U}(\theta,t) = U_c(t)\hat{\mathbf{k}} + \mathbf{U_r}(\theta,t)$, where U_c is the speed of the center of mass, $\hat{\mathbf{k}}$ is the unit vector in the vertical direction, and $\mathbf{U}_\mathrm{r}$ is the velocity of a point in the hoop with respect to the center of mass. See Fig. 1(a) for the coordinate system. The initial translational energy is

$$E_{t,0} = \frac{1}{2} m U_c^2(0), \tag{1}$$

where $t = 0$ indicates the time of takeoff. The initial vibrational energy is $E_{v,0} = (1/2)\int U_r^2(\theta,0)\,\mathrm{d}m$. Because the vibration of the hoop exhibits up-down symmetry upon takeoff and is circular at $t = 0$, we write $\mathbf{U_r}(0,0) = -U_c(0)\hat{\mathbf{k}}$ and $\mathbf{U_r}(\pi,0) = U_c(0)\hat{\mathbf{k}}$. For a thin ring freely vibrating in a plane in its second mode (prolate-oblate shape change), the radial displacement u and the circumferential displacement v are given by $u(\theta,t) = -2B\cos 2\theta \cos(\omega_n t + \epsilon)$ and $v(\theta,t) = B\sin 2\theta \cos(\omega_n t + \epsilon)$, where B is the vibration amplitude, ω_n is the natural frequency, and ϵ is the phase adjustment to match the initial condition.[15] Then $U_r = (\dot{u}^2 + \dot{v}^2)^{1/2} = B\omega_n(4\cos^2 2\theta + \sin^2 2\theta)^{1/2}\cos(\omega_n t)$, where the dot denotes the time derivative. If we use $U_r(\pi,0) = 2B\omega_n = U_c(0)$, we obtain

$$E_{v,0} = \frac{5}{16} m U_c^2(0). \tag{2}$$

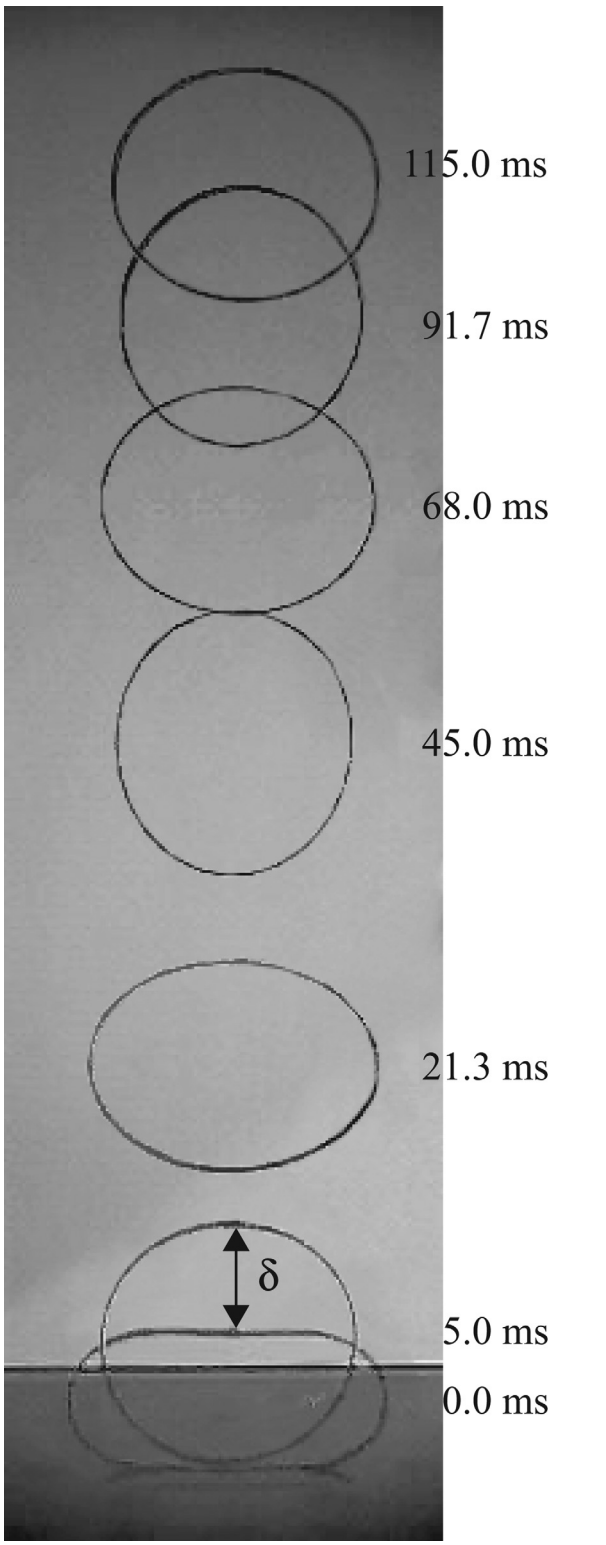

Fig. 2. The jumping sequence of a polyimide hoop with radius $R = 16$ mm, thickness $\tau = 125$ μm, and initial deflection $\delta = 14$ mm.

Because the vibration speed of a hoop scales as $U_r \sim \omega_n \delta$, $\omega_n \sim [(Y/\rho)^{1/2}\tau/R^2]$,[16,17] and $U_r \approx U_c$ at takeoff, both $E_{t,0}$ and $E_{v,0}$ are scaled by $Yw\tau^3\delta^2/R^3$just as is E_b. Also, the ratio $E_{v,0}/E_{t,0}$ is constant, 5/8, due to Eqs. (1) and (2). Our measurements of the positions of the top and bottom of the hoop versus time show that $E_{t,0} \approx 0.57E_b$, as shown in Fig. 3, and the proportionality constant is less than $8/13 \approx 0.62$ due to energy loss to the substrate. Note that the conversion of the initial elastic energy E_b to the initial translational kinetic energy $E_{t,0}$ occurs while the hoop is in contact with the substrate (before takeoff). Thus, the effect of air is ignored. It follows that $E_{v,0} = (5/8)E_{t,0} \approx 0.36E_b$ because of Eqs. (1) and (2), and $E_s \approx 0.07E_b$ by energy conservation. That is, approximately 57 and 36% of the initial elastic strain energy is converted to translational and vibrational energy at take-off, respectively, and the remaining 7% is dissipated in the interaction with the substrate. Although we started with a thin ring approximation ($\tau/R \ll 1$), the vibrational energy of a thick ring was shown[20] to be proportional to the initial strain energy for $\tau/R \lesssim 0.5$, to which our model can be extended.

We now can obtain a crude scaling law for the jump height by balancing $E_{t,0} \sim Yw\tau^3\delta^2/R^3$ with the maximum gravitational potential energy mgH, leading to

$$\frac{H}{h_c} \sim \frac{\tau^2\delta^2}{R^4}, \tag{3}$$

where we used $m = 2\pi\rho R\tau w$ and $h_c = Y/\rho g$, which has the dimension of length. Figure 4 shows the data plotted according to Eq. (3) with a straight line obtained by letting $E_{t,0} = 0.57E_b = mgH$. We see that the discrepancy between theory and experiment grows as H increases, which is due to the energy loss caused by air drag.

IV. EFFECT OF AIR DRAG

We consider the equation of motion of the hoop in the vertical direction,

$$m\dot{U}_c = -mg - D, \tag{4}$$

where the drag $D = C_D\rho_a RwU_c^2$. Here C_D is the drag coefficient and ρ_a is the density of air. We obtained C_D for hoops with different dimensions and velocities in water by measuring the drag force of each hoop at constant speed by a linear translation stage (Newport M-IMS300LM) with a load cell (HBM model SP1). Recall that C_D is a function of the Reynolds number, Re, and geometry only, not the kind of fluid.[21] We found that for $\mathrm{Re} = U_c w/\nu \approx 150$–$1500$, where ν is the kinematic viscosity, which corresponds to the current experimental conditions, $C_D \approx 2.32$ for hoops satisfying $\tau/R < 0.04$. As τ increases further, C_D decreases, in which case a separate measurement of C_D is required. Except for the variation of the numerical values of C_D, our theory holds for $\tau/R \lesssim 0.5$.

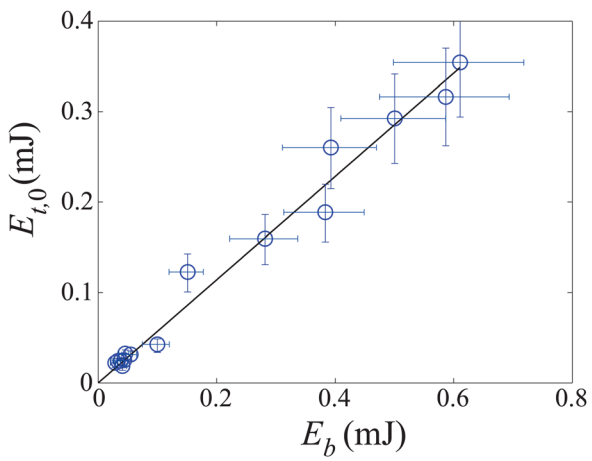

Fig. 3. (Color online) Experimental results for the initial translational kinetic energy $E_{t,0}$ and elastic strain energy E_b, showing their linear relation. The slope of the best fit line is 0.57.

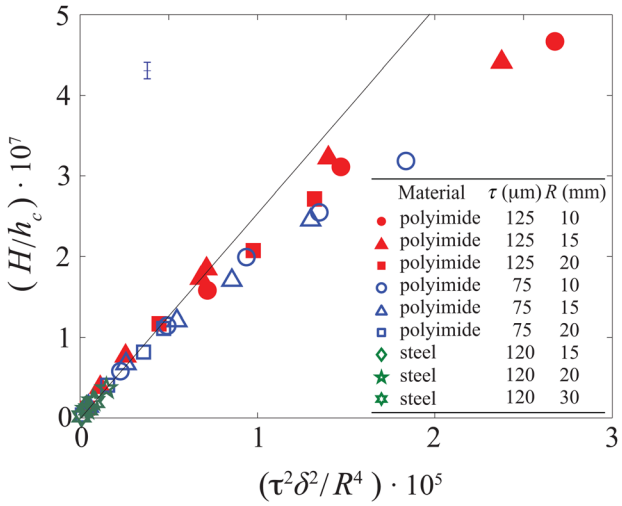

Fig. 4. (Color online) The maximum jumping heights of various hoops with δ ranging up to 12 mm, plotted according to the scaling relation $H/h_c \sim \tau^2\delta^2/R^4$. The straight line corresponds to the jumping height with no air drag obtained by letting $E_{t,0} = 0.57E_b = mgH$. Characteristic error bars are shown in the upper left corner.

By integrating Eq. (4), the hoop velocity $U_c(t)$ is given by,

$$U_c(t) = \sqrt{h_D g}\tan\left(\tan^{-1}\frac{U_0}{\sqrt{h_D g}} - \frac{t}{\sqrt{h_D/g}}\right), \tag{5}$$

where $U_0 = U_c(0)$ and $h_D = 2\pi\rho\tau/\rho_a C_D$. If we integrate $U_c = \dot{h}$ with $h(0) = 0$, we obtain

$$h(t) = h_D \ln\frac{\cos\left[\tan^{-1}(U_0/\sqrt{h_D g}) - t/\sqrt{h_D/g}\right]}{\cos[\tan^{-1}(U_0/\sqrt{h_D g})]}. \tag{6}$$

The initial hoop velocity is related to ω_n and δ. We found experimentally that $U_0 \approx 0.232(Y/\rho)^{1/2}\tau\delta/R^2$. The maximum height of the hoop jump under the effect of air drag, H_a, is obtained by substituting $t = t_{\max} = \sqrt{h_D/g}\tan^{-1}(U_0/\sqrt{h_D g})$, which makes $U_c(t_{\max}) = 0$. From Eq. (6) we have

$$H_a = -h_D \ln\left|\cos\left[\tan^{-1}(0232\sqrt{\phi})\right]\right|, \tag{7}$$

where $\phi = (h_c/h_D)(\tau^2\delta^2/R^4)$. We note that the maximum value of the ratio H_a/h_D depends only on the single parameter ϕ, which can be shown to be $\phi \sim D_0/mg$, where $D_0 = C_D\rho_a RwU_0^2$.

Figure 5(a) shows that the model can accurately predict the time dependence of the hoop height. Figure 5(b) shows that the model collapses all the experimental data for the

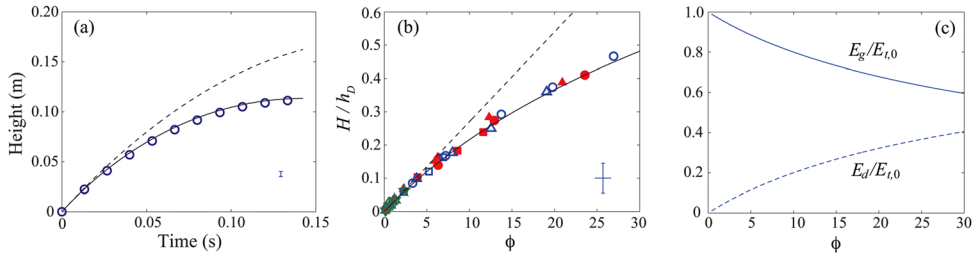

Fig. 5. (Color online) (a) Measured temporal evolution of the height of the hoop with radius $R=15$ mm, thickness $\tau=125$ μm, and initial deflection $\delta=9$ mm (circles) compared to the theories without (dashed line) and with (solid line) air drag. (b) Dimensionless maximum jump height versus ϕ. The solid line is from Eq. (7) and the broken line is drawn by taking $C_D\rightarrow 0$ in Eq. (7). (c) The energy conversion ratio from $E_{t,0}$ to E_g (solid line) and to E_d (dashed line). Characteristic error bars are shown in the lower right corner of (a) and (b).

maximum height onto a single line with the single parameter ϕ. The energy loss due to air drag is $E_d=mg(H_0-H_a)$, where H_0 is the maximum jump height with no air drag. We substitute $E_{t,0}$ of Eq. (1) and $U_c(0)\approx 0.232(Y/\rho)^{1/2}\tau\delta/R^2$ into $H_0=E_{t,0}/mg$ and find $H_0\approx 0.026h_c\tau^2\delta^2/R^4$, which can also be derived by taking $C_D\rightarrow 0$ in Eq. (7) because $\ln\left|\cos\left[\tan^{-1}(0.232\sqrt{\phi})\right]\right|\approx 0.026\phi$ for $\phi\ll 1$.

We plot the ratio $E_d/E_{t,0}=1-H_a/H_0$ and $E_g/E_{t,0}=H_a/H_0$ versus ϕ in Fig. 5(c). The increase of $E_d/E_{t,0}$ and the decrease of $E_g/E_{t,0}$ with ϕ is reasonable because ϕ corresponds to the ratio of the drag to the weight.

V. OPTIMIZATION OF THE HOOP GEOMETRY

We now turn to the optimization of the hoop design and the degree of deformation to maximize H_a in air for a given mass of hoop material. Thanks to the simple relation for H_a in Eq. (7), the optimization is reduced to a simple algebraic problem. We can show that H_a in Eq. (7) depends only on two parameters, τ/R and δ, when Y, w, and $m=2\pi\rho Rw\tau$ are fixed. Because $\partial H_a/\partial(\tau/R)|_\delta>0$ and $\partial H_a/\partial\delta|_{\tau/R}>0$, maximizing both τ/R and δ given various constraints maximizes H_a. We choose three constraints. The first constraint is given by the hoop geometry $\delta<2R-\tau$, which can be expressed as

$$\delta<(R\tau)^{1/2}\left(\frac{\tau}{R}\right)^{-1/2}\left(2-\frac{\tau}{R}\right), \tag{8}$$

where $R\tau$ is fixed. To prevent the yield,[15] or plastic deformation, of the material, we choose the second constraint as $\sigma_{\max}\leq\sigma_y$, where the maximum stress in the hoop $\sigma_{\max}=F[6+38(b/a)^2]/(\pi awR)$, which occurs at the intersection of the inner circumference and the line of action of compressive load,[19] and σ_y is the yield stress. Then δ can be written as

$$\delta<\frac{\pi}{1.12}\frac{\sigma_y\sqrt{R\tau}}{Y}\left(\frac{R}{\tau}\right)^{7/2}\frac{a}{3+19(b/a)^2}, \tag{9}$$

where $a=1+\tau/2R$ and $b=1-\tau/2R$. Because a device that bends the hoop, for example, the leg muscle of an insect or an actuator of a robot, can exert a finite force $F\leq F_{\max}$, the third constraint is given by

$$\delta<\frac{F_{\max}}{0.56Yw(\tau/R)^3}. \tag{10}$$

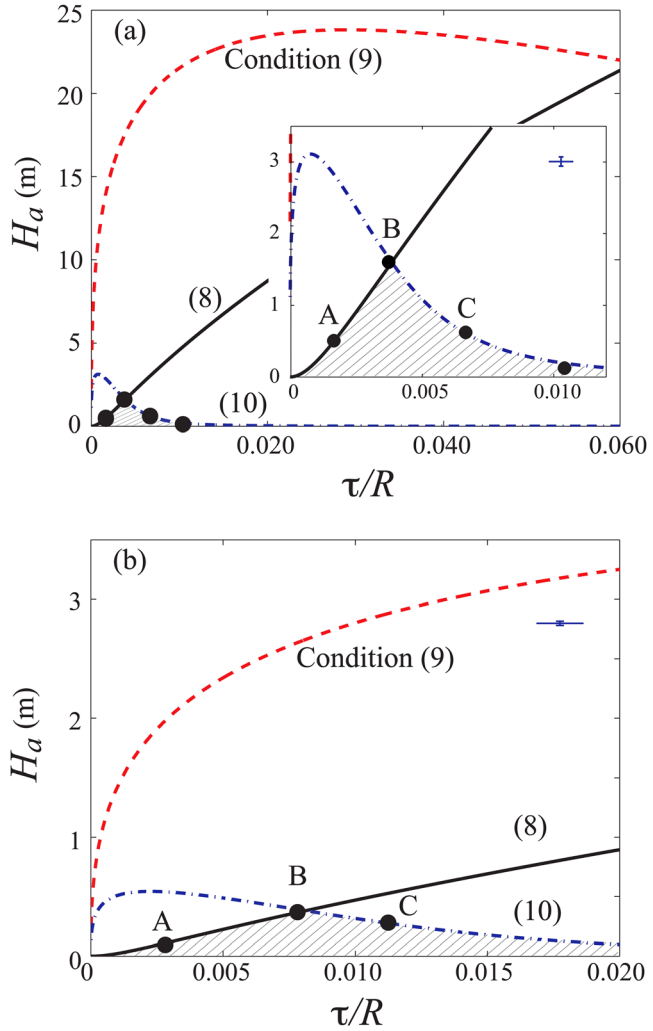

Fig. 6. (Color online) Maximum jump height H_a in air versus τ/R predicted by Eq. (7) corresponding to the conditions of Eqs. (8) (solid line), (9) (dashed line), and (10) (alternate long and short dashed line). All three conditions are satisfied in the hatched area. The filled circles represent experimental results. (a) Steel hoops. Inset: Magnified view around the optimum. (b) Polyimide hoops. Point A: initially the upper segment of a hoop touches the lower one, but the compressive force is lower than the maximum allowable actuator force $F_{\max}$. Point B: initially the hoop bends until its upper segment touches the lower one, at which point the compressive force reaches $F_{\max}$. Point C: the hoop is compressed with the maximum allowable actuator force $F_{\max}$, but the upper segment does not touch the lower one. Characteristic error bars are shown in the upper right corner.

Because all three constraints give the maximum allowable δ as functions of τ/R, a single parameter τ/R can be tuned to optimize H_a in Eq. (7).

Figure 6 shows examples of the optimization results using steel and polyimide hoops. We set $F_{\max} = 1.5$ and 0.1 N, $R\tau = 6 \times 10^{-6}$ m^2 and 2×10^{-6} m^2 for steel and polyimide, respectively, to restrict the jumping height within the laboratory space. For both cases, Eqs. (8) and (10) define the maximum jump height for varying τ/R due to the high strength of the materials. For the point designated as A in Figs. 6(a) and 6(b), the hoop can be initially compressed until its upper segment touches the lower one while still satisfying Eqs. (9) and (10). For point C, the hoop can be initially bent up to a point where the compressive force reaches $F_{\max}$. Point B, where the conditions (8) and (10) coincide, gives the maximum jump height and thus the optimal value of τ/R. Figure 6 also shows that our experiments agree well with theory.

VI. CONCLUSIONS

The jumps of an elastic hoop were analyzed by a combination of experiment and theory. A remarkable result is that a constant percentage (57%) of the initial elastic strain energy, independent of the thickness, radius, initial deflection, and material properties of the hoop, is used to raise the hoop, provided that $\tau/R < 0.5$ and the initial gravitational sagging is ignored. If we consider the effects of drag, we find that the maximum jump ratio H/h_D is a function of the single parameter ϕ [see Eq. (7)], which corresponds to the ratio of the initial air drag to the weight. For a given hoop mass the condition for achieving the maximum jump height is determined by the single parameter τ/R, the ratio of the thickness to the radius of a hoop. We used a constant value of the drag coefficient $C_D = 2.32$ for a fixed hoop width w, which is verified experimentally to be valid for $\tau/R < 0.04$. For thicker hoops, C_D was observed to decrease, which results in a greater jump height than predicted. The optimal value of τ/R is not affected by the value of C_D.

Our theory for the dynamics of the model jumper enables us to treat the jump of various other geometries such as slender beams and hollow shells. A topic of biophysical interest is the shape and dimension of a semilunar process, consisting of chitin fibers in a protein matrix,[22] which is responsible for storing elastic energy in the legs of jumping insects such as a locust,[23] to see whether it has evolved to maximize the jumping efficiency. Also the jumps of various objects on a flexible substrate, which will dissipate more than 7% of the initial elastic strain energy for a rigid substrate, is of interest for understanding insect jumps on plant leaves and on water.[5,6,24]

ACKNOWLEDGMENTS

This work was supported by the National Research Foundation of Korea (Grant Nos. 2009-0082824 and 2010-0029613), and administered via SNU-IAMD. We are grateful to Professor L. Mahadevan for stimulating discussions.

[a]Electronic address: hyk@snu.ac.kr

[1]M. Burrows, "Froghopper insects leap to new heights," Nature (London) **424**, 509 (2003).
[2]M. Burrows and O. Morris, "Jumping and kicking in bush crickets," J. Exp. Biol. **206**, 1035–1049 (2003).
[3]H. C. Bennet-Clark and E. C. A. Lucey, "The jump of the flea: A study of the energetics and a model of the mechanism," J. Exp. Biol. **47**, 59–76 (1967).
[4]H. C. Bennet-Clark, "The energetics of the jump of the locust *Schistocerca gregaria*," J. Exp. Biol. **63**, 53–83 (1975).
[5]D.-G. Lee and H.-Y. Kim, "Impact of a superhydrophobic sphere onto water," Langmuir **24**, 142–145 (2008).
[6]D. L. Hu and J. W. M. Bush, "The hydrodynamics of water-walking arthropods," J. Fluid Mech. **644**, 5–33 (2010).
[7]Y. Sugiyama and S. Hirai, "Crawling and jumping by a deformable robot," Int. J. Robot. Res. **25**, 603–620 (2006).
[8]B. Shin, H.-Y. Kim, and K.-J. Cho, "Towards a Biologically Inspired Small-Scale Water Jumping Robot," in *IEEE International Conference Biomedical Robotics Biomechatronics* (Scottsdale, AZ, 2008), pp. 127–131.
[9]M. Rothschild, J. Schlein, K. Parker, C. Neville, and S. Sternberg, "The jumping mechanism of *Xenopsylla Cheopis* III. Execution of jump and activity," Philos. Trans. R. Soc. London, Ser. B **271**, 499–515 (1975).
[10]W. J. Heitler, "The locust jump. Specialisations of the metathoracic femoral-tibial joint," J. Comp. Physiol. **89**, 93–104 (1974).
[11]M. Burrows, "Morphology and action of the hind leg joints controlling jumping in froghopper insects," J. Exp. Biol. **209**, 4622–4637 (2006).
[12]G. P. Sutton and M. Burrows, "Biomechanics of jumping in the flea," J. Exp. Biol. **214**, 836–847 (2011).
[13]M. Burrows and H. Wolf, "Jumping and kicking in the false stick insect *Prosarthria teretrirostris*: Kinematics and motor control," J. Exp. Biol. **205**, 1519–1530 (2002).
[14]M. E. G. Evans, "The jump of the click beetle (Coleoptera, Elateridae)—a preliminary study," J. Zool. **167**, 319–336 (1972).
[15]A. E. H. Love, *A Treatise on the Mathematical Theory of Elasticity*, 4th ed. (Dover, New York, 1927).
[16]R. Hoppe, "The bending vibration of a circular ring," Crelle J. Math. **73**, 158–170 (1871).
[17]J. L. Lin and W. Soedel, "On general in-plane vibrations of rotating thick and thin rings," J. Sound Vib. **122**, 547–570 (1988).
[18]P. S. Raux, P. M. Reis, J. W. M. Bush, and C. Clanet, "Rolling ribbons," Phys. Rev. Lett. **105**, 044301 (2010).
[19]D. W. Hobbs, "An assessment of a technique for determining the tensile strength of rock," Brit. J. Appl. Phys. **16**, 259–268 (1965).
[20]J. Kirkhope, "In-plane vibration of a thick circular ring," J. Sound Vib. **50**, 219–227 (1977).
[21]G. K. Batchelor, *An Introduction to Fluid Dynamics* (Cambridge U. P., Cambridge, 1967).
[22]P. R. Shewry, A. S. Tatham, and A. Bailey, *Elastomeric Proteins* (Cambridge U. P., Cambridge, 2003).
[23]M. Burrows and G. Morris, "The kinematics and neural control of high-speed kicking movements in the locust," J. Exp. Biol. **204**, 3471–3481 (2001).
[24]J. Brackenbury and H. Hunt, "Jumping in springtails: Mechanism and dynamics," J. Zool. **229**, 217–236 (1993).